Proceedings of Anticancer Research, 2026, Volume 10, Issue 3
http://ojs.bbwpublisher.com/index.php/PAR
Online ISSN: 2208-3553
Print ISSN: 2208-3545

Spatial Mapping Reveals an Immunosuppressive Niche Linking CD8A$^+$ T-cell Exhaustion and Breast Cancer Stem Cells in HER2-Positive Breast Cancer

Fanyi Zhang[1], Li Zhu[1]*, Huijing Yin[2]*

[1]Department of General Surgery, Shanghai General Hospital, Shanghai Jiao Tong University School of Medicine, Shanghai 200120, China
[2]Precision Research Center for Refractory Diseases, Institute for Clinical Research, Shanghai General Hospital, Shanghai Jiao Tong University School of Medicine, Shanghai 200120, China

Authors to whom correspondence should be addressed.

Abstract: *Objective*: This study aimed to characterize the spatial distribution of CD8A$^+$PD-1$^+$TIGIT$^+$ exhausted T cells in HER2-positive breast cancer and to investigate their spatial relationship with CD44$^+$CD24$^-$ breast cancer stem cells. *Method*: Formalin-fixed paraffin-embedded HER2-positive breast cancer specimens were analyzed using multiplex immunofluorescence, pathological region annotation, and spatial proteomic analysis. Regions of interest were annotated based on histological features, including invasive carcinoma-associated areas, adjacent stroma, peritumoral fibrous tissue, and adipose tissue. CD8A$^+$PD-1$^+$TIGIT$^+$ T cells were identified at the single-cell level, and their regional distribution was quantitatively compared. Spatial mapping, distance-based analysis, and interaction network analysis were performed to evaluate the spatial association between exhausted T cells and CD44$^+$CD24$^-$ BCSCs. Pairwise comparisons were conducted using two-tailed Welch's t-test. *Result*: CD8A$^+$PD-1$^+$TIGIT$^+$ T cells were preferentially enriched in invasive carcinoma-associated regions and adjacent stromal areas, with significantly lower abundance in peritumoral fibrous and adipose tissues. Within the CD8A$^+$ T-cell compartment, the proportion of triple-positive exhausted T cells was highest in invasive lesions and decreased toward peripheral non-invasive regions. Spatial analyses showed that CD8A$^+$PD-1$^+$TIGIT$^+$ T cells and CD44$^+$CD24$^-$ BCSCs were co-enriched in invasive carcinoma, tumor–stromal interface zones, and lymphoid tissue-associated microregions. Distance-based heatmaps and interaction network analyses further confirmed recurrent spatial proximity between these two cell populations. *Conclusion*: CD8A$^+$PD-1$^+$TIGIT$^+$ exhausted T cells are spatially enriched in invasive pathological microregions of HER2-positive breast cancer and show close spatial association with CD44$^+$CD24$^-$ BCSCs. The observed spatial overlap between tumor stemness and T-cell exhaustion defines a localized suppressive niche. This interplay likely underpins the biological mechanisms through which HER2-positive breast cancer evades immune surveillance and develops resistance to therapy.

Keywords: HER2-positive breast cancer; T-cell exhaustion; Breast cancer stem cells; Spatial proteomics;

Online publication: May 31, 2026

1. Introduction

Characterized by HER2 protein overexpression or gene amplification, the HER2-positive subtype represents approximately 15–20% of all breast cancer diagnoses. While the clinical landscape has been transformed by HER2-targeted therapies, ranging from monoclonal antibodies to antibody-drug conjugates and tyrosine kinase inhibitors, treatment success is often hindered by both primary and secondary resistance [1]. Increasingly, the tumor immune microenvironment is recognized as a pivotal factor governing these therapeutic outcomes.

Unlike many other breast cancer variants, the HER2-positive subtype is often characterized by a more robust immune landscape. The presence of tumor-infiltrating lymphocytes, particularly $CD8^+$ T cells, frequently aligns with better clinical outcomes and a stronger response to anti-HER2 treatments [2]. This synergy is partly explained by the fact that HER2 antibodies do not just block signaling; they also engage the immune system via mechanisms such as antibody-dependent cellular cytotoxicity (ADCC). This interplay establishes a clear biological foundation for pairing HER2 inhibitors with immunotherapies [3,4].

Antitumor immunity is largely orchestrated by immune checkpoint pathways, which maintain the balance between activation and suppression. PD-1, for instance, drives T-cell impairment and exhaustion when it interacts with its ligands, PD-L1 or PD-L2, on activated T cells. Similarly, TIGIT functions as a critical inhibitory marker on exhausted $CD8^+$ T cells, regulatory T cells, and NK cells [5]. It curtails effector responses by outcompeting CD226 for binding to shared ligands CD155 and CD112, thereby facilitating immune evasion [6]. Because PD-1 and TIGIT are frequently co-expressed during T-cell dysfunction, targeting both pathways simultaneously may offer a more potent strategy for revitalizing immune surveillance than inhibiting either alone [7].

Standard analytical tools often fail to capture the full immune complexity of HER2-positive tumors. While H&E staining defines histological structure, it cannot assess the functional status or checkpoint co-expression of infiltrating lymphocytes. Conversely, bulk transcriptomic and proteomic profiling offer high molecular resolution but sacrifice spatial context. This limitation is critical in breast cancer, where pronounced regional heterogeneity means that immune landscapes can vary significantly within a single lesion [8]. Consequently, resolving these spatial dynamics requires advanced approaches that integrate molecular depth with anatomical integrity.

Spatial proteomic platforms, such as multiplex immunofluorescence, bridge the gap between high-dimensional molecular profiling and tissue morphology by detecting multiple markers in situ [9]. These technologies facilitate the precise quantification of immune subsets, checkpoint densities, and exhaustion phenotypes within pathologically defined zones. By mapping these localized immunosuppressive niches, these platforms provide a critical framework for identifying and selecting rational therapeutic targets in HER2-positive breast cancer [10].

To resolve the spatial architecture of T-cell exhaustion in HER2-positive breast cancer, we integrated multiplex immunofluorescence with pathological annotation and spatial interaction analysis. We characterized the distribution of $CD8A^+PD\text{-}1^+TIGIT^+$ exhausted T cells across distinct compartments,

including invasive carcinoma, stroma, and peritumoral fibrous or adipose tissues, while evaluating their proximity to $CD44^{+}CD24^{-}$ breast cancer stem cells (BCSCs). By combining regional quantification with spatial network analysis, we sought to delineate localized immunosuppressive niches and provide evidence for a spatial link between T-cell exhaustion and the BCSC-enriched microenvironment.

2. Materials and methods

2.1. Clinical specimens

FFPE specimens from HER2-positive breast cancer patients were utilized for both pathological assessment and spatial proteomic analysis. Corresponding clinicopathological data (e.g., age, tumor size, metastasis, grade, stage, and molecular markers such as ER/PR/HER2/Ki-67) were extracted from hospital pathology reports. This study received approval from the local Ethics Committee and adhered to the ethical principles for human subject research. Written informed consent was secured from all patients prior to enrollment.

2.2. Pathology methods

All hematoxylin and eosin-stained and immunohistochemically stained slides were reviewed by two experienced pathologists. Histological type, tumor grade, invasive tumor components, lymph node status, and pathological stage were evaluated according to standard breast cancer pathological criteria. Tumor histological grade was assessed using the Elston and Ellis scoring system. Immunohistochemical staining for ER, PR, HER2, and Ki-67 was performed on 4-μm formalin-fixed paraffin-embedded tissue sections according to routine clinical protocols. ER and PR positivity was defined as nuclear staining in ≥ 1% of tumor cells. HER2 status was scored as 0, 1^{+}, 2^{+}, or 3^{+} by immunohistochemistry, and fluorescence in situ hybridization was performed for cases with equivocal HER2 expression. HER2 positivity was defined as IHC 3^{+} or HER2 gene amplification by fluorescence in situ hybridization. The Ki-67 index was calculated as the percentage of positively stained tumor nuclei in invasive tumor areas. All pathological and immunohistochemical features were assessed based on the invasive tumor components.

For spatial proteomic analysis, representative tumor regions were selected on the basis of corresponding hematoxylin and eosin-stained sections. Regions of interest were annotated by pathologists to include invasive tumor areas and relevant tumor microenvironment regions, while areas with necrosis, tissue folding, poor fixation, or obvious artifacts were excluded.

2.3. Multiplex immunohistochemistry

Multiplex immunohistochemistry/immunofluorescence staining was performed on formalin-fixed paraffin-embedded breast cancer tissue sections. After deparaffinization, rehydration, antigen retrieval, and blocking, sections were sequentially incubated with primary antibodies against immune and functional markers, including CD8, PD-1, TIGIT, and other markers in the panel. Each staining cycle was followed by horseradish peroxidase-conjugated secondary antibody incubation, tyramide signal amplification, and antibody stripping before the next marker was applied. After all staining cycles, nuclei were counterstained with DAPI, and slides were mounted with antifade medium.

Multispectral images were acquired using a fluorescence imaging system. Single-stained controls were used to establish the spectral library and perform spectral unmixing. The unmixed images were subsequently used for tissue segmentation, cell segmentation, phenotyping, and spatial analysis. CD8-positive T cells co-

expressing PD-1 and/or TIGIT were identified at the single-cell level and analyzed within pathologically annotated regions of interest.

2.4. Spatial proteomics

The general process of spatial proteomics is shown in **Figure 1**. Regions of interest were first found in Phenochart and then analysed in inForm to conduct spectral unmixing, tissue segmentation, cell segmentation and phenotype assignment. Export images of the components and cell-level outputs, such as marker intensities, tissue classifications, cell coordinates and phenotype annotations, for further spatial analysis.

Unmixed images were then imported into QuPath for image stitching and data organisation. Manually annotated tissue compartments and performed cell segmentation using StarDist. Based on the pattern of marker expression and morphology, trained object classifiers were used to assign cell phenotypes. QuPath's spatial analysis functions were then used to measure and plot the distance between selected cell populations, such as $CD8^+$ T cells and PD-1- or TIGIT-expressing subsets.

QuPath was used to analyse cell-level data in CytoMAP further for neighbourhood studies. Neighborhoods were defined as 50-μm raster-scanned windows, and the relative abundance of each cell phenotype was quantified within these neighborhoods. Some areas have been divided according to the type of cells. Then, neighborhood composition heatmaps and interaction networks were used to study the spatial distribution and relationships among immune cells in regional associations of tumours to build models of the tumour microenvironment.

2.5. Statistics

Statistical analyses were performed to compare the proportion of $CD8A^+PD\text{-}1^+TIGIT^+$ exhausted T cells among different regions of interest. Data are presented as mean ± standard deviation. Pairwise comparisons between ROI groups were conducted using a two-tailed Welch's t-test, which does not assume equal variance between groups. Statistical significance is indicated as $*P < 0.05$.

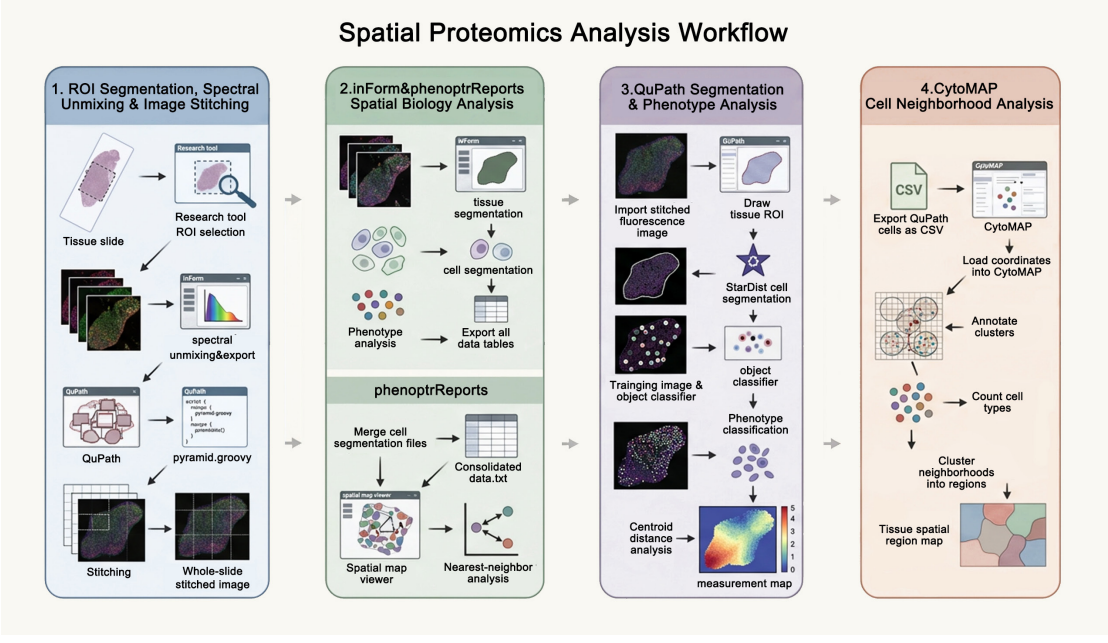

Figure 1. The overall workflow of spatial proteomic analysis.

3. Results

3.1. Spatial enrichment of $CD8A^+PD\text{-}1^+TIGIT^+$ T cells in invasive pathological microregions of HER2-positive breast cancer

To assess whether T-cell exhaustion varies across regions of the HER2-positive breast cancer tumor microenvironment, we first focused on the $CD8A^+PD\text{-}1^+TIGIT^+$ T-cell subset. $CD8A^+$ T cells are major mediators of cytotoxic antitumor immunity, whereas PD-1 and TIGIT are inhibitory receptors closely associated with exhaustion-related immune suppression. Their co-expression on $CD8A^+$ T cells may therefore indicate a more advanced exhausted phenotype. On this basis, we analyzed the spatial distribution of this cell population across pathologically distinct microregions.

A representative tumor section from a patient with HER2-positive breast cancer was selected for analysis. Based on histological architecture and pathological features, the section was divided into three regions of interest (ROIs). ROI1 mainly contained invasive carcinoma intermingled with stromal components. ROI2 included invasive carcinoma and stroma, with multifocal lymphocytic infiltration and areas of lymphoid tissue hyperplasia. ROI3 was composed primarily of peritumoral fibrous and adipose tissue. Multiplex immunofluorescence staining for CD8A, PD-1, and TIGIT was then performed to detect $CD8A^+PD\text{-}1^+TIGIT^+$ triple-positive cells, together with other $CD8A^+$ T-cell phenotypes (**Figures 2A–C**).

In this representative section, $CD8A^+PD\text{-}1^+TIGIT^+$ T cells accounted for the largest proportion in ROI1, decreased in ROI2, and were least frequent in ROI3 (**Figure 2D**). Further phenotypic stratification of the $CD8A^+$ T-cell compartment showed that triple-positive cells represented a relatively enriched subset in ROI1, whereas $CD8A^+PD\text{-}1^-TIGIT^-$ cells were more prominent in ROI3 (**Figure 2E**). These findings suggest that regions associated with invasive carcinoma may not only attract $CD8A^+$ T cells but also preferentially contain cells co-expressing PD-1 and TIGIT, consistent with a locally enhanced exhausted phenotype.

The region-specific pattern observed in the representative case was further examined in pathological sections from six additional patients with HER2-positive breast cancer. Quantitatively, $CD8A^+PD\text{-}1^+TIGIT^+$ T cells were significantly more concentrated in ROI1, and then decreased step-wise in ROI2 and ROI3 (**Figure 2F**). Analysis of the composition of $CD8A^+$ T cells showed a similar trend: the fraction of triple-positive cells decreased from the invasive carcinoma-associated region to the peritumoral tissue, and $CD8A^+PD\text{-}1^-TIGIT^-$ cells showed a relative increase in the opposite direction (**Figure 2G**). Based on the above results, $CD8A^+PD\text{-}1^+TIGIT^+$ T cells are not uniformly distributed in the tumour microenvironment. Instead, they are more likely to be located in invasive carcinoma-associated microregions, and thus support the existence of a spatially organised pattern of T-cell exhaustion in HER2-positive breast cancer.

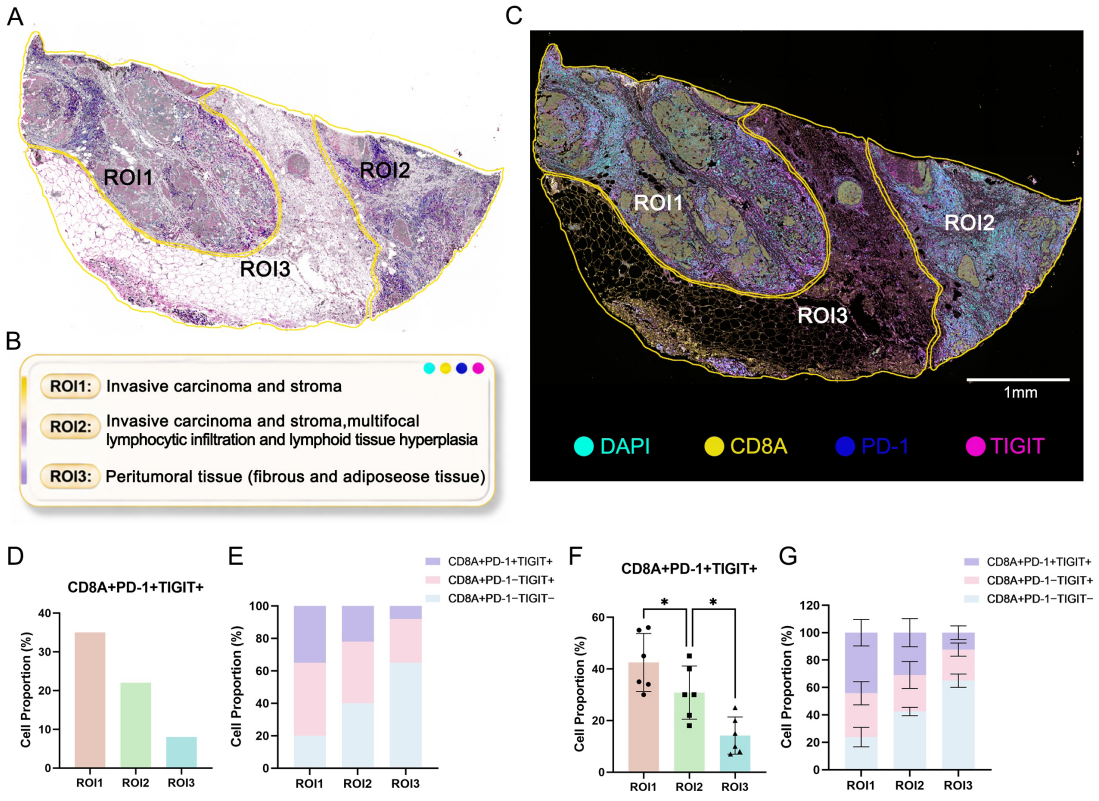

Figure 2. Spatial Enrichment of CD8A$^+$PD-1$^+$TIGIT$^+$ T Cells in Invasive Pathological Microregions of HER2-Positive Breast Cancer.(A) Panoramic view of a representative pathological section from a HER2-positive breast cancer patient, divided into three regions of interest (ROIs) according to histological architecture. (B) Summary of pathological features of the three ROIs. (C) Multiplex immunofluorescence image of the representative section showing DAPI, CD8A, PD-1, and TIGIT staining, together with the spatial locations of the three ROIs. Scale bar, 1 mm. (D) Proportion of CD8A$^+$PD-1$^+$TIGIT$^+$ cells in the three ROIs of the representative section. (E) Phenotypic composition of CD8A$^+$ T-cell subsets in the three ROIs of the representative section, including CD8A$^+$PD-1$^+$TIGIT$^+$, CD8A$^+$PD-1$^-$TIGIT$^+$, and CD8A$^+$PD-1$^-$TIGIT$^-$ cells. (F) Quantitative analysis of the proportion of CD8A$^+$PD-1$^+$TIGIT$^+$ cells across the three ROIs in pathological sections from six HER2-positive breast cancer patients. (G) Compositional analysis of CD8A$^+$ T-cell phenotypes across the three ROIs in six HER2-positive breast cancer patients. Data are presented as mean ± SEM. *P < 0.05.

3.2. CD8A$^+$PD-1$^+$TIGIT$^+$ T cells and CD44$^+$CD24$^-$ breast cancer stem cells are spatially co-enriched in invasive lesions

After observing the preferential accumulation of CD8A$^+$PD-1$^+$TIGIT$^+$ T cells in invasive carcinoma-associated regions, we next evaluated whether this exhausted T-cell subset was spatially associated with specific tumor cell niches. The CD44$^+$CD24$^-$ phenotype is widely used to identify breast cancer stem-like cells and has been associated with tumor invasion, recurrence, treatment resistance, and immune escape [11,12]. We therefore analyzed the spatial relationship between CD8A$^+$PD-1$^+$TIGIT$^+$ T cells and CD44$^+$CD24$^-$ BCSCs in the same HER2-positive breast cancer section, to determine whether cancer stem-like cell-enriched areas were accompanied by local enrichment of exhausted T cells.

Panoramic spatial mapping showed that neither CD8A$^+$PD-1$^+$TIGIT$^+$ T cells nor CD44$^+$CD24$^-$ BCSCs were uniformly distributed in the tissue section. Instead, both groups were mainly clustered in areas of

invasive carcinoma and the adjacent stroma (**Figure 3A**). On the other hand, the adipose- and fibre-poor area far from the tumour parenchyma was relatively sparse. A distance-based spatial heatmap also shows that the intercellular distance is shorter between the two groups, specifically in invasive carcinoma and the surrounding stromal area, indicating that these pathological micro-regions are closer in space (**Figure 3B**). The above distribution indicates that the regional accumulation of $CD8A^{+}PD\text{-}1^{+}TIGIT^{+}$ T cells is unlikely to be due to general inflammation; instead, it may be linked to a specific microenvironment in that area with certain types of cancer cells.

High-magnification observation of individual areas also confirmed the above. In ROI1, $CD8A^{+}PD\text{-}1^{+}TIGIT^{+}$ T cells and $CD44^{+}CD24^{-}$ BCSCs were mainly co-distributed in the invasive carcinoma lesions and adjacent stromal areas, with a prominent accumulation at the interface among tumor parenchyma, lymphocyte-enriched regions, and fibrous stroma (**Figures 3C, D, F, G**). Although the tissue architecture in ROI2 was more heterogeneous, both populations were still mainly restricted to invasive carcinoma and marginal tumor regions, and they were in close spatial proximity at the tumor-stroma interface (**Figures 3E, H, I, L**). In several other representative subregions, the two cell populations were similarly enriched near invasive carcinoma lesions and adjacent stroma, and their abundance was significantly reduced in adipose tissue and fibrous areas away from the tumor parenchyma (**Figures 3J, K, M, N**).

Based on the above results, it can be concluded that $CD8A^{+}PD\text{-}1^{+}TIGIT^{+}$ T cells and $CD44^{+}CD24^{-}$ BCSCs are spatially co-enriched in HER2-positive breast cancer, primarily located in invasive carcinoma, tumor-stromal interface zones, and lymphoid tissue-associated microregions. Therefore, the spatial arrangement may create a niche for cancer stem-cell-enriched cells that induces local immune exhaustion, and together the two will constitute an immunosuppressive pathological microenvironment.

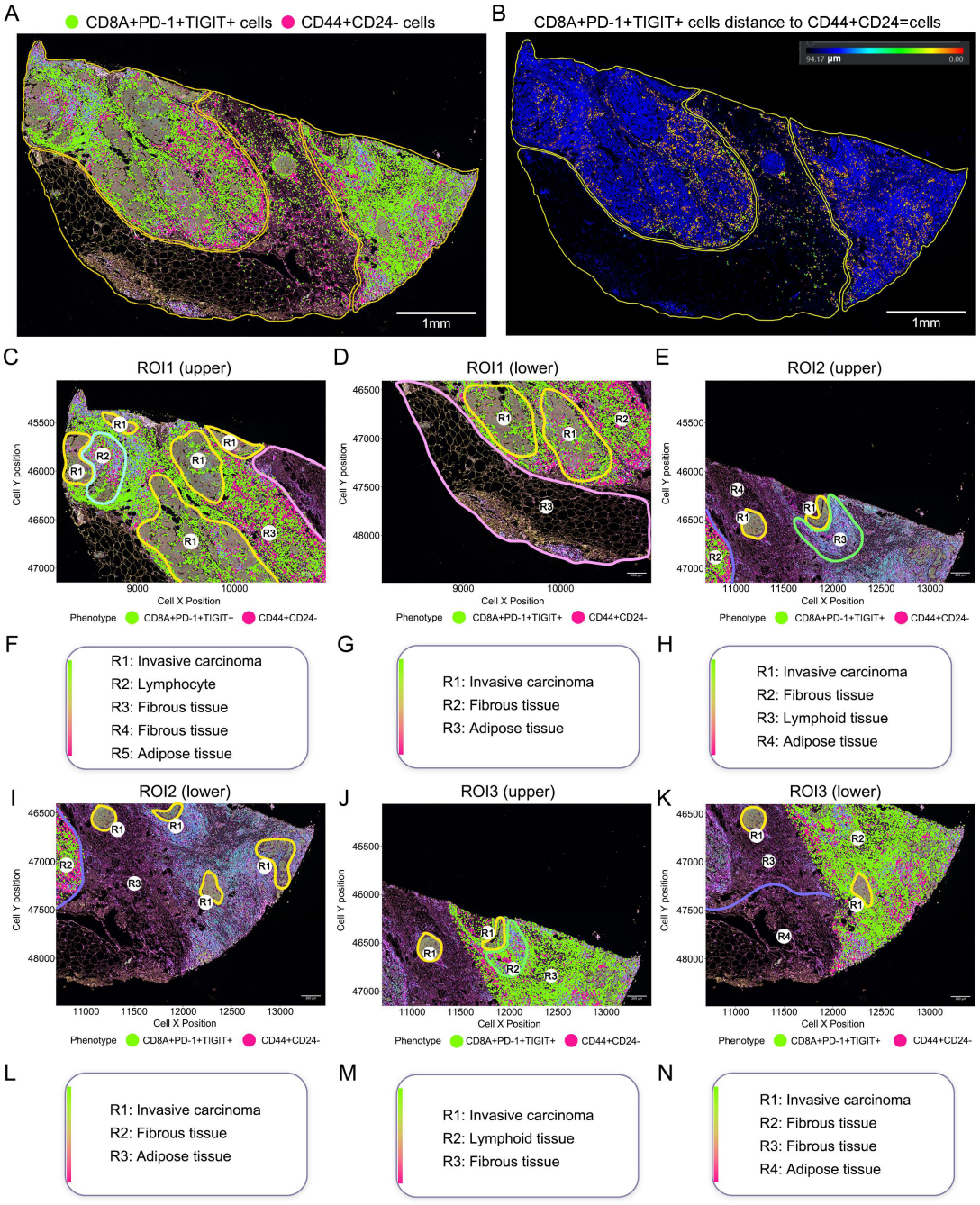

Figure 3. CD8A^{+}PD-1^{+}TIGIT^{+} T cells and CD44^{+}CD24^{-} breast cancer stem cells are spatially co-enriched in invasive lesions.(A) Panoramic spatial distribution of CD8A^{+}PD-1^{+}TIGIT^{+} T cells and CD44^{+}CD24^{-} BCSCs in a representative HER2-positive breast cancer section. Fluorescent green indicates CD8A^{+}PD-1^{+}TIGIT^{+} T cells, and magenta indicates CD44^{+}CD24^{-} BCSCs. Scale bar, 1 mm. (B) Distance-based spatial heatmap showing the proximity between the two cell populations. Warmer colors indicate shorter distances, whereas cooler colors indicate greater distances. Scale bar, 1 mm. (C–E, I–K) Magnified representative regions from ROI1 and ROI2 showing the spatial distribution of the two cell populations across invasive carcinoma, lymphoid/lymphocyte-enriched areas, fibrous tissue, and adipose tissue. Scale bars, 200 µm. (F–H, L–N) Corresponding pathological annotations for the magnified regions shown in C–E and I–K.

3.3. Spatial interaction network analysis further confirms the proximity between $CD8A^+PD\text{-}1^+TIGIT^+$ T Cells and $CD44^+CD24^-$ breast cancer stem cells

Building on the observation that $CD8A^+PD\text{-}1^+TIGIT^+$ T cells and $CD44^+CD24^-$ BCSCs are co-enriched, we wanted to know if this co-distribution represented a close, measurable association. Therefore, a spatial interaction network and matrix analysis were conducted on multiple ROIs. The study models the distances between cells as network edges and matrix-based affinity scores to systematically compare the spatial relationships among exhausted T cells, BCSCs, and other cellular components in the microenvironment.

Both subregions in ROI1 showed a clear spatial proximity of the two cell types (**Figures 4A–B**). Interaction matrices have quantified these associations and revealed positive interaction signals and self-aggregation in the exhausted $CD8A^+$ T-cell compartment (**Figures 4D, E**). Given that the interaction signals are stronger in the lower subregion, it is estimated that the spatial interface of exhausted T cells and BCSCs may be context-dependent and influenced by heterogeneous histological structures within the tumour.

Parallel spatial patterns were observed in ROI2, and both subregions were close to exhausted T cells and BCSCs (**Figures 4C, G**). Quantitative analysis of interaction matrices also shows that these areas are not spatially segregated in terms of tissue structure (**Figures 4F, J**). The reappearance of this pattern, especially the enhanced signal in the lower subregion, indicates that the association between $CD8A^+PD\text{-}1^+TIGIT^+$ T cells and BCSCs is a conserved trait of the HER2-positive tumor microenvironment.

Spatial connectivity of the two populations still existed in the peritumoral area of ROI3 (**Figures 4H, I**). The lower subregion showed an enhanced interaction between exhausted $CD8A^+$ T cells and $CD44^+CD24^-$ BCSCs (**Figures 4K, L**). In conjunction with the results from tumour-rich areas, these data indicate that the exhausted T cell-BCSC axis is a ubiquitous feature of the microenvironment and remains spatially organized independently of changes in local tumour cell concentration or stromal abundance.

In short, based on our spatial interaction network and matrix analysis, it has been found that $CD8A^+PD\text{-}1^+TIGIT^+$ T cells and $CD44^+CD24^-$ BCSCs are in proximity in all areas of the histological microregion. Based on the above data, it can be concluded that exhausted T cells and cancer stem-like cells in HER2-positive breast cancer are in contact.

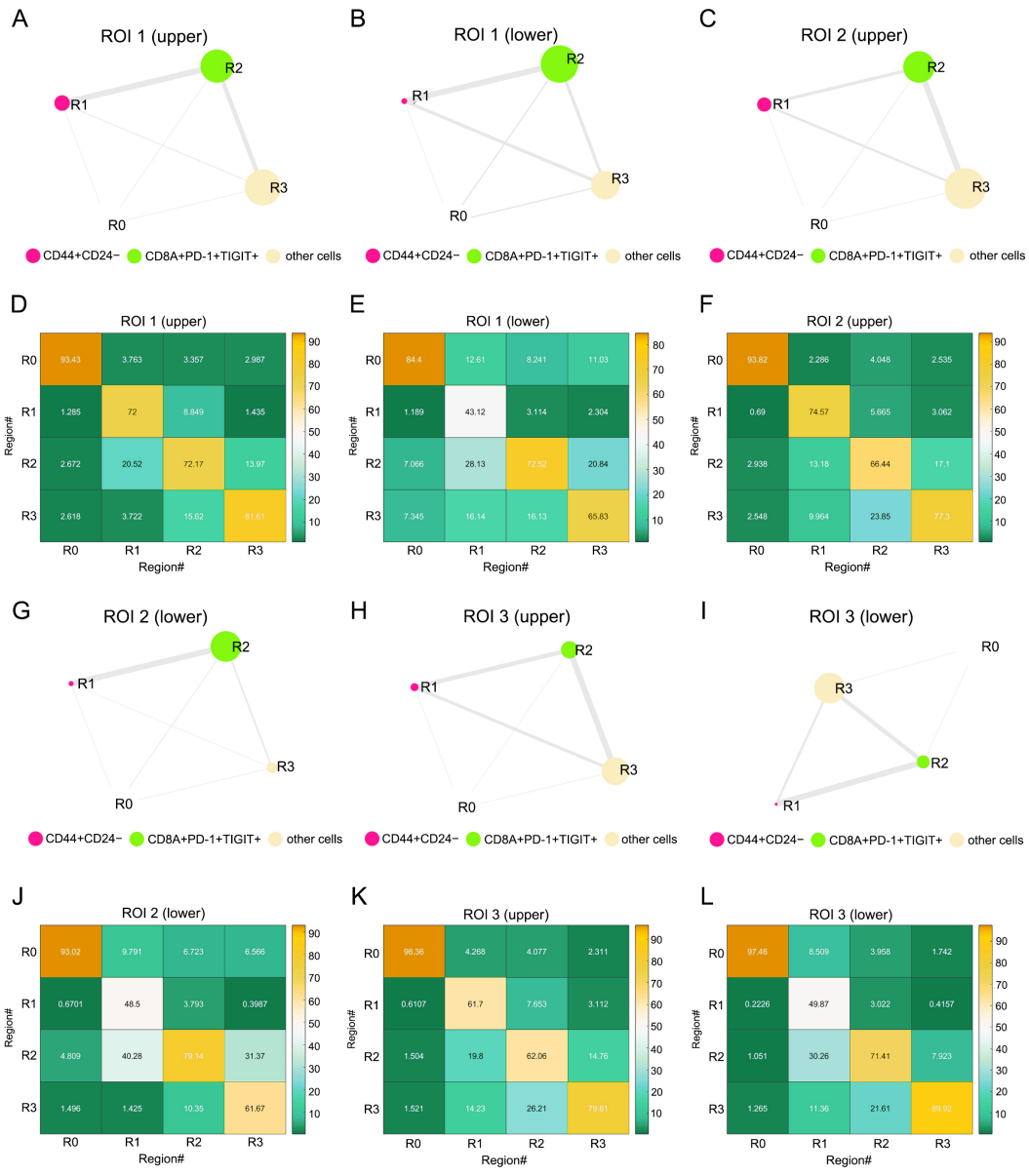

Figure 4. Spatial interaction network analysis further confirms the proximity between CD8A^{+}PD-1^{+}TIGIT^{+} T cells and CD44^{+}CD24^{-} breast cancer stem cells.(A–C, G–I) Spatial interaction networks generated from local regions of ROI1–ROI3 shown in Figure 2. Magenta nodes indicate CD44^{+}CD24^{-} BCSCs, fluorescent green nodes indicate CD8A^{+}PD-1^{+}TIGIT^{+} T cells, and pale-yellow nodes indicate other cells. Node size represents the relative abundance of each cell population, and edge thickness indicates interaction strength. (D–F, J–L) Corresponding spatial interaction matrices. Values and color intensity indicate the degree of spatial proximity between cell populations, with yellow representing stronger interactions and green representing weaker interactions. R1, CD44^{+}CD24^{-} BCSCs; R2, CD8A^{+}PD-1^{+}TIGIT^{+} T cells; R3, other cells; R0, unclassified/background cell populations.

4. Discussion

Multiplex immunofluorescence combined with computational spatial models was used to show that the enrichment of CD8A^{+}PD-1^{+}TIGIT^{+} T cells is not random but strictly confined to the invasive front of

the tumor-stroma, and they are significantly lacking in the surrounding fibro-adipose tissue. The core of this spatial organisation is the strong link among exhausted T cells and $CD44^{+}CD24^{-}$ BCSCs, and this association also occurs in many types of tissue structures. As shown in **Figure 5**, our proposed model of "exhaustion zoning" can divide the tumour microenvironment into multiple areas with differing degrees of immunosuppression. In short, the above results indicate that the BCSC-exhausted T cell axis is a relatively isolated and self-sustaining immunosuppressive area that can lead to treatment failure.

The conventional interpretation of $CD8A^{+}$ T-cell density as a surrogate for active immunity is challenged by the localized exhaustion signature identified in this study [13]. Despite their enrichment in invasive regions, these $CD8A^{+}$ T cells predominantly exhibit a $PD\text{-}1^{+}TIGIT^{+}$ phenotype, indicative of a compromised functional state [14]. Therefore, despite a high level of infiltration in HER2-positive tumours, it may not be indicative of immune cell activity but rather a local area of immune suppression. The above observations suggest that, at present, only cell counting is being performed; we need to consider all dimensions of distribution and function to conduct a more comprehensive analysis of immune cell infiltration.

Based on our analysis, there is a non-random spatial proximity between exhausted $CD8A^{+}$ T cells and BCSCs, and this is not due to individual tissue differences. Therefore, the co-occurrence of these two in the high-risk pathological area suggests that cancer stemness and immune exhaustion are not independent phenomena but are functionally related at this site. Thus, such a space is likely to offer a favourable environment for tumour survival under immune pressure. By finding this repeated connection, our research supports the hypothesis that BCSCs can organise a localised immunosuppressive environment and thus protect the regenerative centre of the tumour from effective T-cell-mediated elimination, contributing to the aggressive clinical behaviour of HER2-positive breast cancer [15].

The first is the application of space-time analysis to observe changes in the immune microenvironment of tissues at a high resolution in this paper. Non-spatial assays combine signals from various cell types; on the other hand, a spatial framework can identify cellular "neighborhoods" precisely [16]. Through triangulation of results from wide-area distribution patterns, local ROI deep dives and network-based proximity metrics, consistent evidence has been provided for the spatial coupling of exhausted T cells and BCSCs. Based on the above data, immunosuppression is inherently a localised phenomenon that presents as a high-risk area of abnormal immune microenvironment rather than an even distribution throughout the whole tumour.

Based on the above data, it is proposed that, in the clinical application of HER2-positive breast cancer treatment, a dual strategy of targeting tumour stemness and reversing immune exhaustion should be adopted simultaneously, rather than focusing on only one of these pathways. Notably, the spatial co-enrichment of $CD8A^{+}PD\text{-}1^{+}TIGIT^{+}$ T cells with $CD44^{+}CD24^{-}$ BCSCs has provided a microanatomical basis for exploring combination regimens that integrate anti-HER2 agents, stemness pathway inhibitors, and dual immune checkpoint blockade of PD-1 and TIGIT.

This study has several limitations that should be noted. The cohort size was relatively small, and the spatial distributions reported here await validation in larger, independent patient populations. Additionally, spatial proximity between cell populations does not, by itself, establish direct intercellular communication or causality. Mechanistic dissection through spatial transcriptomics, single-cell RNA sequencing, ligand–receptor interaction modeling, and functional assays will be required in subsequent work. It should also be recognized that although the $CD44^{+}CD24^{-}$ immunophenotype is commonly employed as a surrogate for breast cancer stemness, its biological significance in this particular setting would benefit from corroboration using alternative stemness markers and functional validation experiments.

Taken together, our data reveal that $CD8A^{+}PD\text{-}1^{+}TIGIT^{+}$ exhausted T cells preferentially accumulate within invasive pathological microregions of HER2-positive breast cancer, where they reside in consistent spatial

proximity to $CD44^{+}CD24^{-}$ BCSCs. These observations provide spatially resolved evidence linking local tumor stemness features with T-cell dysfunction, and point toward this immunosuppressive microenvironment as a potentially important determinant of immune evasion and treatment resistance in HER2-positive disease.

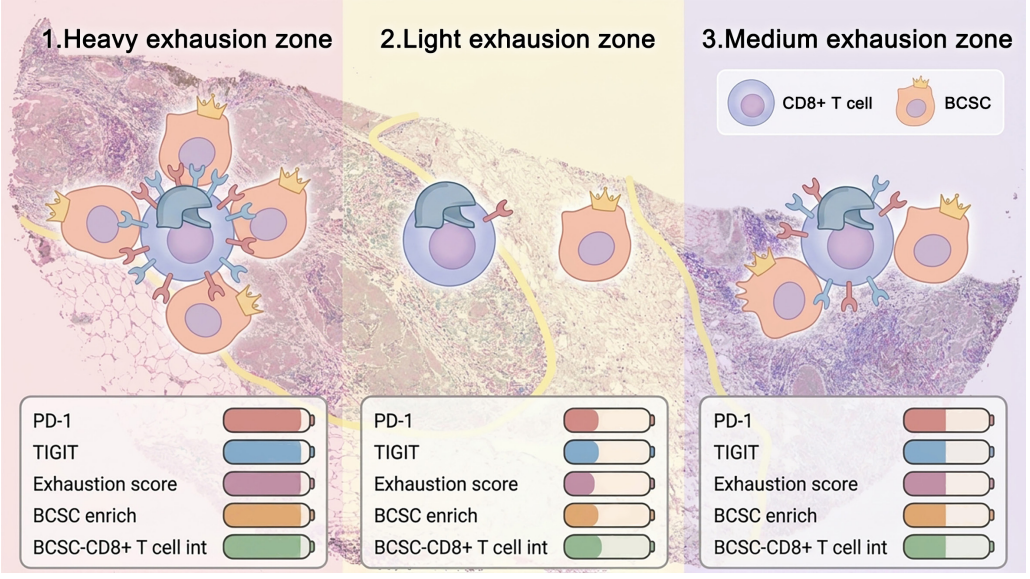

Figure 5. Schematic model illustrating spatially heterogeneous immune-exhaustion niches in HER2-positive breast cancer.

5. Conclusion

In conclusion, this study demonstrates that $CD8A^{+}PD\text{-}1^{+}TIGIT^{+}$ T cells are preferentially enriched in invasive pathological regions of HER2-positive breast cancer and show stable spatial proximity to $CD44^{+}CD24^{-}$ breast cancer stem-like cells. These findings suggest that tumor stemness and T-cell exhaustion may be locally coupled within distinct microenvironmental niches. Our results provide spatial evidence for a region-specific immunosuppressive landscape in HER2-positive breast cancer and offer a basis for future investigation into combined therapeutic strategies targeting both cancer stemness and immune exhaustion.

Funding

National Natural Science Foundation of China (Project No.: 81601985, 82173171, 82372904)

Disclosure statement

The authors declare no conflict of interest.

References

[1] Paz-Manrique R, Pinto JA, Gomez Moreno HL, 2025, Antibody-Drug Conjugates (ADCs) for Breast Cancer Therapeutic Landscape: Concept and Mechanisms of Action. Hematology/Oncology and Stem Cell Therapy,

18(4): 133–139.

[2] Philip M, Schietinger A, 2022, CD8+ T Cell Differentiation and Dysfunction in Cancer. Nature Reviews Immunology, 22(4): 209–223.

[3] Emens LA, Esteva FJ, Beresford M, et al., 2020, Trastuzumab Emtansine Plus Atezolizumab Versus Trastuzumab Emtansine Plus Placebo in Previously Treated, HER2-Positive Advanced Breast Cancer (KATE2): A Phase 2, Multicentre, Randomised, Double-Blind Trial. The Lancet Oncology, 21(10): 1283–1295.

[4] Huober J, Barrios CH, Niikura N, et al., 2022, Atezolizumab With Neoadjuvant Anti–Human Epidermal Growth Factor Receptor 2 Therapy and Chemotherapy in Human Epidermal Growth Factor Receptor 2–Positive Early Breast Cancer: Primary Results of the Randomized Phase III IMpassion050 Trial. Journal of Clinical Oncology, 40(25): 2946–2956.

[5] Chauvin JM, Zarour HM, 2020, TIGIT in Cancer Immunotherapy. Journal for Immunotherapy of Cancer, 8(2): e000957.

[6] Cai L, Li Y, Tan J, et al., 2023, Targeting LAG-3, TIM-3, and TIGIT for Cancer Immunotherapy. Journal of Hematology & Oncology, 16: 101.

[7] Chu X, Tian W, Wang Z, et al., 2023, Co-Inhibition of TIGIT and PD-1/PD-L1 in Cancer Immunotherapy: Mechanisms and Clinical Trials. Molecular Cancer, 22: 93.

[8] Risom T, Glass DR, Averbukh I, et al., 2022, Transition to Invasive Breast Cancer Is Associated With Progressive Changes in the Structure and Composition of Tumor Stroma. Cell, 185(2): 299–310.e18.

[9] Jackson HW, Fischer JR, Zanotelli VRT, et al., 2020, The Single-Cell Pathology Landscape of Breast Cancer. Nature, 578(7796): 615–620.

[10] Wu SZ, Al-Eryani G, Roden D, et al., 2021, A Single-Cell and Spatially Resolved Atlas of Human Breast Cancers. Nature Genetics, 53(9): 1334–1347.

[11] Al-Hajj M, Wicha MS, Benito-Hernandez A, et al., 2003, Prospective Identification of Tumorigenic Breast Cancer Cells. Proceedings of the National Academy of Sciences of the United States of America, 100(7): 3983–3988.

[12] Creighton CJ, Li X, Landis M, et al., 2009, Residual Breast Cancers After Conventional Therapy Display Mesenchymal as Well as Tumor-Initiating Features. Proceedings of the National Academy of Sciences of the United States of America, 106(33): 13820–13825.

[13] Loi S, Michiels S, Salgado R, et al., 2014, Tumor Infiltrating Lymphocytes Are Prognostic in Triple Negative Breast Cancer and Predictive for Trastuzumab Benefit in Early Breast Cancer: Results From the FinHER Trial. Annals of Oncology, 25(8): 1544–1550.

[14] Johnston RJ, Comps-Agrar L, Hackney J, et al., 2014, The Immunoreceptor TIGIT Regulates Antitumor and Antiviral CD8+ T Cell Effector Function. Cancer Cell, 26(6): 923–937.

[15] Miranda A, Hamilton PT, Zhang AW, et al., 2019, Cancer Stemness, Intratumoral Heterogeneity, and Immune Response Across Cancers. Proceedings of the National Academy of Sciences, 116(18): 9020–9029.

[16] Keren L, Bosse M, Marquez D, et al., 2018, A Structured Tumor-Immune Microenvironment in Triple Negative Breast Cancer Revealed by Multiplexed Ion Beam Imaging. Cell, 174(6): 1373–1387.e19.